

NANO EXPRESS

Open Access

A new method to disperse CdS quantum dot-sensitized TiO₂ nanotube arrays into P3HT:PCBM layer for the improvement of efficiency of inverted polymer solar cells

Fumin Li¹, Chong Chen^{1*}, Furui Tan¹, Gentian Yue¹, Liang Shen² and Weifeng Zhang¹

Abstract

We report that the efficiency of ITO/nc-TiO₂/P3HT:PCBM/MoO₃/Ag inverted polymer solar cells (PSCs) can be improved by dispersing CdS quantum dot (QD)-sensitized TiO₂ nanotube arrays (TNTs) in poly (3-hexylthiophene) and [6,6]-phenyl-C₆₁-butyric acid methyl ester (P3HT:PCBM) layer. The CdS QDs are deposited on the TNTs by a chemical bath deposition method. The experimental results show that the CdS QD-sensitized TNTs (CdS/TNTs) do not only increase the light absorption of the P3HT:PCBM layer but also reduce the charge recombination in the P3HT:PCBM layer. The dependence of device performances on cycles of CdS deposition on the TNTs was investigated. A high power conversion efficiency (PCE) of 3.52% was achieved for the inverted PSCs with 20 cyclic depositions of CdS on TNTs, which showed a 34% increase compared to the ITO/nc-TiO₂/P3HT:PCBM/MoO₃/Ag device without the CdS/TNTs. The improved efficiency is attributed to the improved light absorbance and the reduced charge recombination in the active layer.

Keywords: Inverted; Polymer solar cells; Nanotube; Quantum dot

Background

Polymer solar cells (PSCs) have gained great interest because of their low cost, flexibility, and abundant availability [1-7]. So far, the high power conversion efficiency (PCE) of PSCs is achieved by bulk heterojunction (BHJ) PSCs composed of electron-donating polymers and electron-accepting fullerenes [8]. Although significant progress has been made on the improvement of the PCE of PSCs in recent years, the efficiency of the PSCs is still lower than their inorganic counterparts, such as silicon and CIGS. The main factors limiting the efficiency of the PSCs are the low light absorption efficiency due to the narrow absorption band of the absorption spectra of the polymers and the charge recombination in the devices due to the low charge transport efficiency in the electron-donating and electron-accepting materials [9]. To overcome these problems, many efforts have been made on improving the absorption spectra and charge carrier

mobility of the photovoltaic materials for higher PCE [10-13]. Some inorganic nanostructure materials with high light absorption of the visible spectrum and the near infrared spectral range are dispersed in to the polymer:fulleride layer to increase the light absorption such as CdS [14,15], CdSe [16], PbS [17], Sb₂S₃ [18], and FeS₂ [19,20]. In addition, some inorganic materials with high charge carrier mobility, such as ZnO and TiO₂, are used to increase the charge transport efficiency and reduce the charge recombination [21-23]. Specially, because the ordered TiO₂ nanotube arrays (TNTs) possess outstanding charge transport properties, the TNTs are used to reduce the charge recombination in the PSCs and therefore improved the efficiency as reported recently [24]. It is worthy to note that most of these materials are synthesized in advance through complicated chemical method and then dispersed in active layers. Of which, usually, only one type of these inorganic nanostructure materials is dispersed in active layer. However, there are few reports on which two types of inorganic

* Correspondence: mrchenchong@163.com

¹Key Laboratory of Photovoltaic Materials, Department of Physics and Electronics, Henan University, Kaifeng 475004, People's Republic of China
Full list of author information is available at the end of the article

nanostructure materials are compactly combined and dispersed in active layers.

This report focuses on the synthesis of the CdS quantum dot (QD)-sensitized TiO₂ nanotube arrays (CdS/TNTs) in a simple way (chemical bath deposition (CBD)) and dispersion in active layers. CdS QDs help light absorption to produce more excitons and also help to form the interface of CdS/P3HT with P3HT in the P3HT:PCBM layer so that more excitons are separated. TNTs are able to make prompt transfer of the excitons produced by light absorption of CdS QDs. Excitons are separated efficiently enough to reduce the charge recombination. Meanwhile, TNTs are used to form the interface of TNTs/P3HT with P3HT in the active layer and also enhance the separation of excitons. Therefore, CdS/TNTs synthesized using the CBD method and dispersed in P3HT:PCBM layer not only increase the light absorption but also reduce the charge recombination. It is known that few studies on the synthesis of CdS/TNTs using the CBD method to enhance PSCs' PCE are reported.

The result shows that after the CdS/TNTs are dispersed in the P3HT:PCBM layer, the light absorption of the active layer is greatly improved, and the charge recombination is largely controlled. Comparing to the device without CdS/TNTs, the efficiency of the device with CdS/TNTs mentioned above increases by 34%, which fully proves the reasonability of this reported method.

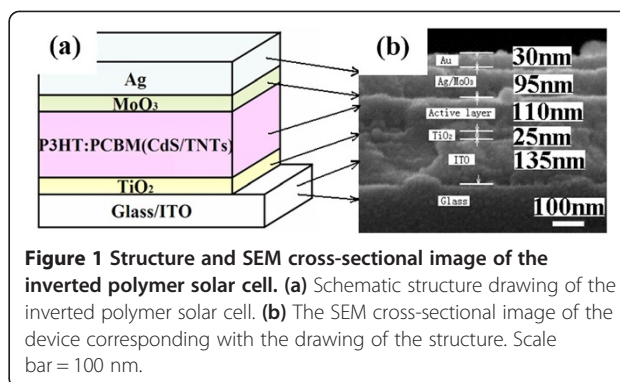
Methods

Fabrication of TNTs

Highly ordered and vertically oriented TNTs were prepared by anodization of Ti (titanium foil, 0.25-mm thickness, 99.7% purity; Sigma-Aldrich, St. Louis, MO, USA) sheets in an electrolyte consisting of 0.25 wt.% ammonium fluoride (NH₄F) (98 + % purity; Sigma-Aldrich) and 0.5 wt.% distilled (DI) water in ethylene glycol (EG) (C₂H₆O₂, 99.0% purity; Sigma-Aldrich) at 40 V for 8 h. A detailed experimental procedure has been described in our previous paper [25]. After anodization, the samples were washed with DI water to remove the occluded ions and dried in a N₂ stream. Finally, the samples were annealed at 450°C for 2 h with a heating rate of 5°C min⁻¹ at ambient conditions.

Synthesis of CdS-coated TNTs

CdS as an inorganic photon absorption material was deposited on TNTs by sequential CBD. Briefly, the as-prepared TNTs were successively immersed in four different beakers for about 40 s each: beakers contained a 50 mM cadmium chloride (CdCl₂) (98.0%; Sigma-Aldrich) aqueous solution and a 50 mM sodium sulfide nonahydrate (Na₂S) (98.0% purity; Sigma-Aldrich) aqueous solution, respectively, and the other two contained DI water to wash the samples to remove the excess of each precursor.



The CBD process was performed by dipping the prepared TNTs in CdCl₂ aqueous solution, rinsing it with DI water, dipping it in Na₂S aqueous solution, followed by a further rinsing with DI water. The two-step dipping procedure is considered as one CBD cycle. After several cycles, the sample became yellow. In this study, 10, 20, and 30 cycles of CdS deposition were performed (denoted as CdS(10), CdS(20), and CdS(30), respectively). The as-prepared samples were dried in a N₂ stream. The TNT sample after *n* cycles of CdS deposition was denoted as CdS(*n*)/TNTs. Finally, the CdS(*n*)/TNT powder was peeled off from the Ti sheets by bending them.

Fabrication of devices

The photovoltaic device has a structure of ITO/nc-TiO₂/P3HT:PCBM (CdS/TNTs)/MoO₃/Ag (P3HT, 95 + % regioregular, electronic grade, Luminescence Technology Co., Hsin-Chu, Taiwan; PCBM, 99.5 + %, Luminescence Technology Co.) as shown schematically in Figure 1a. The ITO-conducting glass substrate (a sheet resistance of 15 Ω/□) was pre-cleaned using acetone, ethanol, and DI water for 15 min each. Anatase phase TiO₂ thin films was prepared as described in our previous papers [26,27]. The thickness

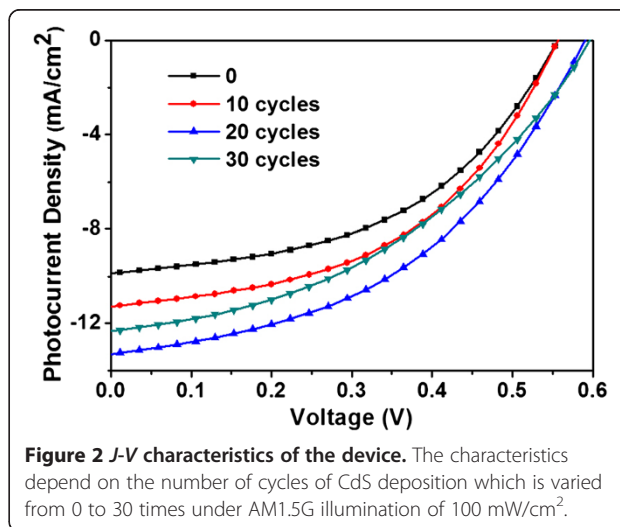


Table 1 Characteristic data of inverted polymer solar cells with different cycles of CdS deposition on TNTs

Cycles	J_{sc} (mA/cm ²)	V_{oc} (V)	FF (%)	PCE (%)	R_s (Ω)
0	9.84	0.56	48.12	2.63	32.6
10	11.29	0.56	47.63	3.01	33.5
20	13.31	0.59	48.81	3.52	30.2
30	12.28	0.60	41.13	3.04	44.9

of TiO₂ is 25 nm. P3HT (used as received) was dissolved in 1,2-dichlorobenzene to produce an 18-mg/ml solution, followed by blending with PCBM (used as received) in 1:1 weight ratio [28]. The blend was divided into four equal parts after being stirred for 72 h in air. Then, the same quality of CdS(*n*)/TNTs (*n* = 10, 20, 30) powder was dispersed in the blend to produce a 1-mg/ml solution, respectively. Simultaneously, there was one equal part which did not contain CdS(*n*)/TNTs (denoted as CdS(0)/TNTs). The blend was ultrasonically disrupted for 2 h in air and then was continuously stirred before spin coating on top of the TiO₂ film surface. Then, the samples were baked in low vacuum (vacuum oven) at 150°C for 10 min. The typical film thickness of P3HT:PCBM (CdS(*n*)/TNTs) was about 100 nm. Finally, 1 nm of MoO₃ and 100 nm of Ag were thermally evaporated in sequence under high vacuum (5×10^{-4} Pa) without disrupting the vacuum. The deposition rate was about 0.05 nm/s, which was monitored with a quartz-oscillating thickness monitor (CRTM-9000, ULVAC, Methuen, MA, USA). These thicknesses could be observed from Figure 1b that shows the cross-section of a typical device by scanning electronic microscope (SEM). It was noticed that there was about 30 nm of Au sputtered on the surface of the sample, as seen on SEM. The active area of the device was about 4 mm².

Characterization and measurements

Current density-voltage (*J-V*) characteristics were measured using a computer-programmed Keithley 2400 sourcemeter (Cleveland, OH, USA) under AM1.5G solar illumination using a Newport 94043A solar simulator (Jiangsu, China). The intensity of the solar simulator was 100 mW/cm².

Light intensity was corrected by a standard silicon solar cell. The transmission and reflection spectra were measured using ultraviolet/visible (UV-vis) spectrometer (Cary 5000, Agilent Technologies Inc., Santa Clara, CA, USA).

Results and discussion

Figure 2 shows the *J-V* characteristics of the inverted PSCs when cycles of CdS deposition vary from 0 to 30 times under AM1.5G illumination of 100 mW/cm². The detailed results are given in Table 1. The control sample device (without CdS(*n*)/TNTs) shows a short-circuit current density (J_{sc}) of 9.84 mA/cm², open-circuit voltage (V_{oc}) of 0.56 V, fill factor (FF) of 48.12%, and PCE of 2.63%. When the CdS depositions are 20 cycles, the photovoltaic device has a J_{sc} of 13.31 mA/cm², V_{oc} of 0.56 V, FF of 48.81%, and PCE of 3.52%. The J_{sc} of the device with 0 cycles is the smallest, and the J_{sc} of the device with 20 cycles is the largest. It shows a 34% efficiency increase compared to the control sample device. It is possible for the limited absorbing ability of P3HT:PCBM. When depositing CdS(*n*)/TNT powder in the blend, the performance has improved remarkably because of its good light absorption properties and electron transport capacity. When the CdS deposition is 30 cycles, the J_{sc} of the photovoltaic device reduces to 12.28 mA/cm², while FF and PCE reduce as well. It can be interpreted that the bigger size of the CdS/TNT powders rather than the fewer cycles can depress their degree of dispersion in the blend after too many depositions. As a result, the film formation of the device is not good, and the series resistance of the device increases. It is well known that the series resistance greatly affects the fill factor and efficiency of solar cells [16]. The main characteristic parameters are slightly reduced.

To investigate whether the CdS/TNTs are evenly dispersed in the blend, the surface SEM images of a typical device is shown in Figure 3 at different scale bars. Figure 3a shows the image of the device at a scale bar of 1 μ m. It can be clearly seen that after ultrasonic disruption and magnetic stirring, PCBM blended with the CdS/TNT powders, and then after spin coating, the

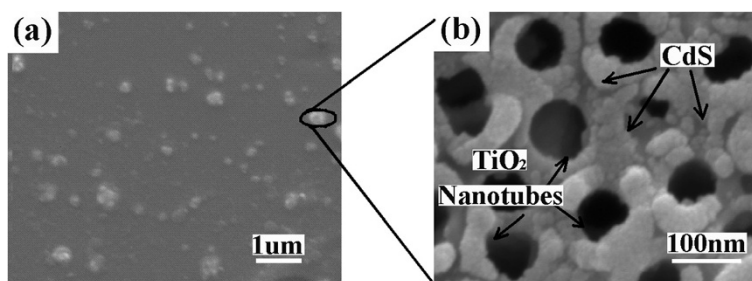


Figure 3 SEM surface image of a typical device. (a) The SEM surface image of a typical device; scale bar, 1 μ m. **(b)** Regional enlargement image of the CdS/TNTs; scale bar, 100 nm.

CdS/TNT powders are distributed on the surface of active layer. To see the details, Figure 3b shows the regional enlargement image of the CdS/TNTs at a scale bar of 100 nm. The CdS is well coated on the surface of the TNTs. The two types of inorganic nanostructure materials are compactly combined and dispersed in active layers uniformly.

Figure 4 shows the UV-vis absorption spectra and the corresponding transmission spectra of the inverted PSCs with 20 cycles (device II) and without CdS(*n*)/TNTs (device I) between the wavelengths 350 and 700 nm. Obviously, after the CdS(*n*)/TNTs deposition, the absorption of the device II films appears around 400 to 650 nm. The absorbance of the spectra of the CdS(*n*)/TNTs films increases significantly not only in the UV region but also in the visible region, which is mainly due to the CdS(*n*)/TNT light absorption within the 350- to 500-nm excitation spectral range. It can be seen that the device II has a wider absorption range and a stronger absorption intensity than device I. CdS/TNTs are suitable for absorption enhancement of photovoltaic application.

Figure 5 compares the incident photon-to-current collection efficiency (IPCE) spectrum of devices fabricated with and without the CdS(*n*)/TNT deposition in the active layer. The IPCE is defined as the number of photo-generated charge carrier contributing to the photocurrent per incident photon. The conventional device (without the CdS(*n*)/TNTs) shows the typical spectral response of the P3HT:PCBM composites with a maximum IPCE of approximately 50% at 500 nm, consistent with the previous studies [29,30]. For device II (with the CdS(*n*)/TNTs), the results demonstrate a substantial enhancement of approximately 10% in the IPCE less than the 500 nm excitation spectral range. The reason for this phenomenon may be due to the increased light absorption, which can be seen from Figure 4. On one hand,

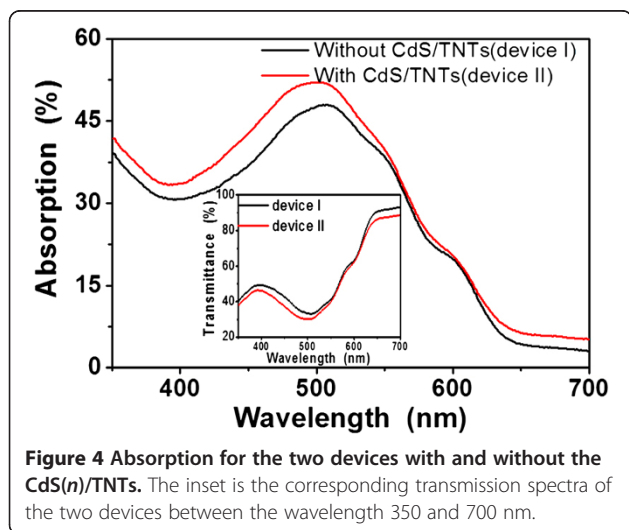


Figure 4 Absorption for the two devices with and without the CdS(*n*)/TNTs. The inset is the corresponding transmission spectra of the two devices between the wavelength 350 and 700 nm.

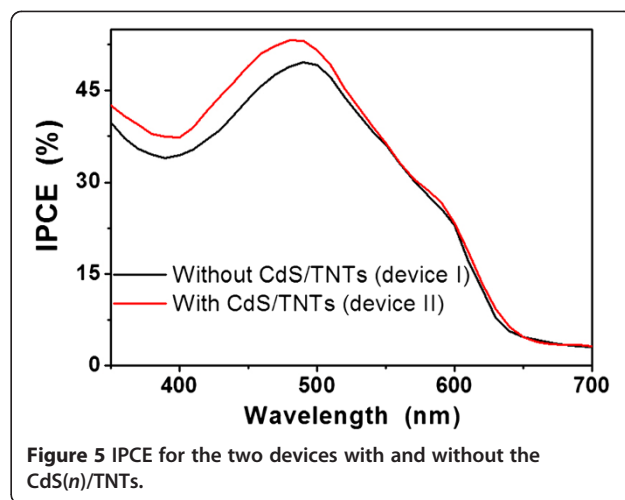


Figure 5 IPCE for the two devices with and without the CdS(*n*)/TNTs.

the increased light absorption due to the introduction of the CdS/TNT powder led to more generated electrons. On the other hand, the introduction of the CdS/TNT powders resulted in a larger exciton-dissociation interface area, such as CdS/P3HT and TNTs/P3HT interfaces, which may lead to a more efficient dissociation efficiency of excitons generated in the active layer.

Conclusions

In summary, we demonstrated a new method which significantly improves the solar cells' efficiency which could be obtained via simply dispersing compactly combined CdS/TNTs in an active layer. The CdS/TNTs were synthesized by sequential chemical bath deposition. As a result, a high PCE of 3.52% was achieved for the inverted PSCs with 20 cycles of CdS, which showed a 34% increase compared to conventional P3HT:PCBM devices. We believe that this is a simple but effective method that can be used to improve the efficiency of polymer solar cells.

Competing interests

The authors declare that they have no competing interests.

Authors' contributions

FL carried out the experiments, participated in the sequence alignment, and drafted the manuscript. CC participated in the device preparation. FT, GY, LS, and WZ were involved in the SEM, UV-vis, and IPCE analysis of the devices. All authors read and approved the final manuscript.

Acknowledgements

This work was supported by the National Natural Science Foundation of China (Grant No. 61306019), the Education Department Foundation of Henan Province (Grant No. 14A430022), the Science Foundation of Henan University (Grant No. 2013YBZR049), and Henan University Distinguished Professor Startup Fund.

Author details

¹Key Laboratory of Photovoltaic Materials, Department of Physics and Electronics, Henan University, Kaifeng 475004, People's Republic of China. ²Department of Electronic Science and Engineering, Jilin University, Changchun 130012, People's Republic of China.

Received: 14 March 2014 Accepted: 24 April 2014
Published: 16 May 2014

References

1. Sariciftci NS, Smilowitz L, Heeger AJ, Wudl F: Photo induced electro transfer from a conducting polymer to buckminsterfullerene. *Science* 1992, **25**:1474–1476.
2. Kim JY, Lee K, Coates NE, Moses D, Nguyen TQ, Dante M, Heeger AJ: Efficient tandem polymer solar cells fabricated by all-solution processing. *Science* 2007, **317**:222–225.
3. Chen HY, Hou JH, Zhang SQ, Liang YY, Yang GW, Yang Y, Yu LP, Wu Y, Li G: Polymer solar cells with enhanced open-circuit voltage and efficiency. *Nat Photonics* 2009, **3**:649–653.
4. Krebs FC, Nielsen TD, Fyenbo J, Wadstrom M, Pedersen MS: Manufacture, integration and demonstration of polymer solar cells in a lamp for the "lighting Africa" initiative. *Energ Environ Sci* 2010, **3**:512–525.
5. Han KK, Jong WL: Flexible IZO/Ag/IZO/Ag multilayer electrode grown on a polyethylene terephthalate substrate using roll-to-roll sputtering. *Nanoscale Res Lett* 2012, **7**:67.
6. Hansen RMD, Liu YH, Madsen M, Rubahn H: Flexible organic solar cells including efficiency enhancing grating structures. *Nanotechnology* 2013, **24**:145301.
7. Voigt MM, Guite A, Grupp J, Mosley A: Polymer field-effect transistors fabricated by the sequential gravure printing of polythiophene, two insulator layers, and a metal ink gate. *Adv Funct Mater* 2010, **20**:239–246.
8. You JB, Dou LT, Yoshimura K, Kato T, Ohya K, Moriarty T, Emery K, Chen CC, Gao J, Li G, Yang Y: A polymer tandem solar cell with 10.6% power conversion efficiency. *Nat Commun* 2013, **4**:1446.
9. Li YF, Zou YP: Conjugated polymer photovoltaic materials with broad absorption band and high charge carrier mobility. *Adv Mater* 2008, **20**:2952–2958.
10. He Z, Zhong C, Su S, Xu M, Wu H, Cao Y: Enhanced power-conversion efficiency in polymer solar cells using an inverted device structure. *Nat Photonics* 2012, **6**:591–595.
11. Li X, Choy WCH, Huo L, Xie F, Sha WEI, Ding B, Guo X, Li Y, Hou J, You J, Yang Y: Dual plasmonic nanostructures for high performance inverted organic solar cells. *Adv Mater* 2012, **24**:3046–3052.
12. Sun Y, Takacs CJ, Cowan SR, Seo JH, Gong X, Roy A, Heeger AJ: Efficient, air-stable bulk heterojunction polymer solar cells using MoOx as the anode interfacial layer. *Adv Mater* 2011, **23**:2226–2230.
13. Yang TT, Wang M, Duan CH, Hu XW, Huang L, Peng JB, Huang F, Gong X: Inverted polymer solar cells with 8.4% efficiency by conjugated polyelectrolyte. *Energ Environ Sci* 2012, **5**:8208–8214.
14. Khan MT, Bhargava R, Kaur A, Dhawan SK, Chand S: Effect of cadmium sulphide quantum dot processing and post thermal annealing on P3HT/PCBM photovoltaic device. *Thin Solid Films* 2010, **519**:1007–1011.
15. Leventis HC, King SP, Sudlow A, Hill MS, Molloy KC, Haque SA: Nanostructured hybrid polymer-inorganic solar cell active layers formed by controllable *in situ* growth of semiconducting sulfide networks. *Nano Lett* 2010, **10**:1253–1258.
16. Xu TT, Qiao QQ: Conjugated polymer-inorganic semi-conductor hybrid solar cells. *Energ Environ Sci* 2011, **4**:2700–2720.
17. Günesa S, Fritz KP, Neugebauer H, Sariciftcia NS, Kumarb S, Schollesb GD: Hybrid solar cells using PbS nanoparticles. *Sol Energ Mat Sol C* 2007, **91**:420–423.
18. Chang JA, Rhee JH, Im SH, Lee YH, Kim H, Seok SI, Nazeeruddin MK, Gratzel M: High-performance nano-structured inorganic-organic heterojunction solar cells. *Nano Lett* 2010, **10**:2609–2612.
19. Lin CW, Wang DY, Wang YT, Chen CC, Yang YJ, Chen YF: Increased photocurrent in bulk-heterojunction solar cells mediated by FeS₂ nanocrystals. *Sol Energ Mat Sol C* 2011, **95**:1107–1110.
20. Lin YY, Wang DY, Yen HC, Chen HL, Chen CC, Chen CM, Tang CY, Chen CW: Extended red light harvesting in a poly(3-hexylthiophene)/iron disulfide nanocrystal hybrid solar cell. *Nanotechnology* 2009, **20**:405207.
21. Olson DC, Piris J, Collins RT, Shaheen SE, Ginley DS: Hybrid photovoltaic devices of polymer and ZnO nanofiber composites. *Thin Solid Films* 2006, **496**:26–29.
22. Lin YY, Chen CW, Chu TH, Su WF, Lin CC, Ku CH, Wu JJ, Chen CH: Nanostructured metal oxide/conjugated polymer hybrid solar cells by low temperature solution processes. *J Mater Chem* 2007, **17**:4571–4576.
23. Yang P, Zhou X, Cao G, Luscombe CK: P3HT:PCBM polymer solar cells with TiO₂ nanotube aggregates in the active layer. *J Mater Chem* 2010, **20**:2612–2616.
24. Foong TRB, Chan KL, Hu X: Structure and properties of nano-confined poly(3-hexylthiophene) in nano-array/polymer hybrid ordered-bulk heterojunction solar cells. *Nanoscale* 2012, **4**:478–485.
25. Chen C, Ali G, Yoo SH, Kum JM, Cho SO: Improved conversion efficiency of CdS quantum dot-sensitized TiO₂ nanotube-arrays using CuInS₂ as a co-sensitizer and an energy barrier layer. *J Mater Chem* 2011, **21**:16430–16435.
26. Li FM, Ruan SP, Xu Y, Meng FX, Wang JL, Chen WY, Shen L: Semitransparent inverted polymer solar cells using MoO₃/Ag/WO₃ as highly transparent anodes. *Sol Energ Mat Sol C* 2011, **95**:877–880.
27. Tao C, Ruan SP, Zhang XD, Xie GH, Shen L, Kong XZ, Dong W, Liu CX, Chen WY: Performance improvement of inverted polymer solar cells with different top electrodes by introducing a MoO₃ buffer layer. *Appl Phys Lett* 2008, **93**:193307.
28. Shrotriya V, Li G, Yao Y, Moriarty T, Emery K, Yang Y: Accurate measurement and characterization of organic solar cells. *Adv Funct Mater* 2006, **16**:2016–2023.
29. Brabec CJ: Organic photovoltaics: technology and market. *Sol Energ Mat Sol C* 2004, **83**:273–292.
30. Kim JY, Kim SH, Lee HH, Lee K, Ma WL, Gong X, Heeger AJ: New architecture for high-efficiency polymer photovoltaic cells using solution-based titanium oxide as an optical spacer. *Adv Mater* 2006, **18**:572–576.

doi:10.1186/1556-276X-9-240

Cite this article as: Li et al.: A new method to disperse CdS quantum dot-sensitized TiO₂ nanotube arrays into P3HT:PCBM layer for the improvement of efficiency of inverted polymer solar cells. *Nanoscale Research Letters* 2014 **9**:240.

Submit your manuscript to a SpringerOpen[®] journal and benefit from:

- Convenient online submission
- Rigorous peer review
- Immediate publication on acceptance
- Open access: articles freely available online
- High visibility within the field
- Retaining the copyright to your article

Submit your next manuscript at ► springeropen.com